

Cite this: *RSC Mechanochem.*, 2025, 2, 468Received 6th November 2024  
Accepted 20th January 2025

DOI: 10.1039/d4mr00131a

rsc.li/RSCMechanochem

## Stainless-steel-initiated acylation of quinoxalin-2(1*H*)-ones with aldehydes under mechanochemical conditions†

Diandian Wei,‡ Zongwei Li,‡ Heng Li and Bingxin Yuan \*

Utilizing direct mechanocatalytical conditions, we have developed a C–H acylation of quinoxalin-2(1*H*)-one initiated by stainless-steel milling balls. A wide range of functional groups are bearable, affording the desired products in excellent yields. Noteworthy is the short reaction period (30 min) and no requirement for solvent. The late-stage functionalization of pharmaceutical-related molecules illustrates its potential application in drug development. Gram-scale synthesis further demonstrates the scalability and sustainability of this method.

Mechanochemistry has attracted extensive attention in recent years due to its wide application in environmentally friendly methods.<sup>1</sup> Mechanical transformation of small organic molecules using ball milling techniques has emerged as a new area of research in organic synthesis.<sup>2</sup> Compared to traditional solution-based protocols, ball milling offers several advantages, including reduced solvent consumption, shorter reaction times, mild reaction conditions, simple operation, and simplified work-up procedures.<sup>3</sup> In some cases, the milling media can serve as an active catalyst, offering extra advantages such as easy catalyst recovery from the reaction mixture. An early example of this concept was demonstrated by Mack *et al.*, who replaced copper(i) iodide in the Sonogashira reaction with copper balls and jars.<sup>4</sup> Since then, researchers have explored various milling media, including palladium,<sup>5</sup> nickel,<sup>6</sup> copper,<sup>7</sup> and stainless-steel milling media.<sup>8</sup> Among these, stainless steel milling equipment stands out due to its cost-effectiveness and commercial availability. Stainless steel primarily consists of transition metal elements, such as Fe, Cr, and Ni, which are widely utilized in catalytic reactions. Consequently, the use of stainless-steel equipment to initiate reactions, such as the

hydrogenation reaction with water or ether as a hydrogen source,<sup>9</sup> the reduction reaction of nitro or azide to amine,<sup>10</sup> and the addition reaction of sulfoximidoyl chlorides,<sup>11</sup> has gained considerable significance in green chemistry.

Quinoxalin-2(1*H*)-ones represent a significant class of heterocyclic compounds with diverse applications in organic synthesis, materials chemistry, and pharmaceuticals.<sup>12</sup> C3-modified quinoxalin-2(1*H*)-ones are particularly valuable structural motifs found in numerous natural products and drug molecules, exhibiting diverse biological activities, including anticancer, antibacterial, antiviral, and protein kinase inhibitory properties (Scheme 1a).<sup>13</sup> Therefore, a wide range of C3-functionalized quinoxalin-2(1*H*)-ones have been developed through various methods, including arylation, alkylation, acylation, phosphorylation, and amination. Among them, C3-acylation *via* a free radical process is becoming an effective method to prepare C3-acyl quinoxalin-2(1*H*)-ones but remains relatively less explored.

The abstraction of a hydrogen atom from readily available aldehydes to produce acyl radicals has newly come into prominence due to its high atom-economy, benchtop stability, low cost, widespread availability, and no release of halide waste.<sup>14</sup> Several studies have reported the use of *tert*-butyl hydroperoxide (TBHP) as an oxidant in combination with iron salts as catalysts to generate acyl radicals from aldehydes. For instance, Bao and co-workers achieved the production of acyl radicals from aromatic aldehydes using Fe(OTf)<sub>3</sub> and TBHP, requiring 24 hours at room temperature.<sup>15</sup> Meanwhile, Yang and colleagues reported FeCl<sub>2</sub>-catalyzed TBHP-mediated acyl radical generation from aromatic aldehydes, with the reaction performed at 80 °C for 12 hours (Scheme 1b).<sup>16</sup> Qu and colleagues devised a metal-free C3-acylation method for quinoxaline-2(1*H*)-ones with aldehydes in dichloroethane at 70 °C, employing 4 equivalents of TBHP as the oxidizing agent.<sup>17</sup>

Despite these advances, most acylation strategies utilizing aldehydes or other acylation reagents rely on organic solvents, high reaction temperatures, and long reaction times and often exhibit low acylation efficiency, which limits their overall

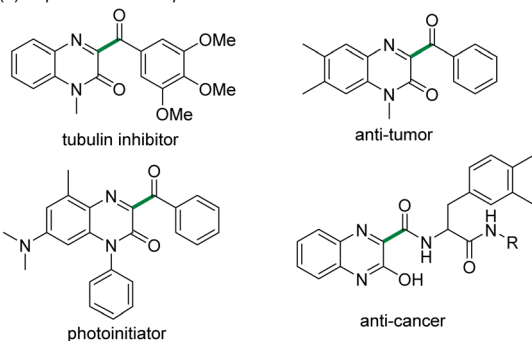
A Green Catalysis Center, College of Chemistry, Zhengzhou University, Zhengzhou, Henan, China, 450001. E-mail: bxyuan@zzu.edu.cn

† Electronic supplementary information (ESI) available: Experimental procedures, characterization data, and <sup>1</sup>H and <sup>13</sup>C NMR spectra. See DOI: <https://doi.org/10.1039/d4mr00131a>

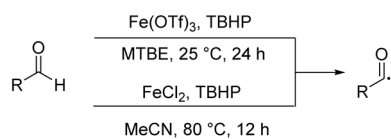
‡ These authors contributed equally to this work.



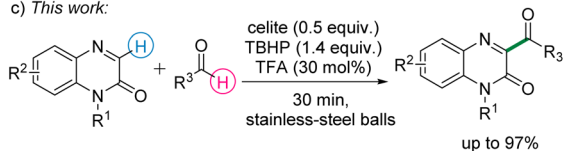
## (a) Representative examples:



## b) Previous examples:



## c) This work:



stainless steel balls-initiated

solvent-free

fast and efficient

gram-scale

Scheme 1 Representative examples and synthetic strategies of C3-acylated quinoxalin-2(1H)-ones.

sustainability and efficiency. Notably, the accumulation of organic waste in chemical manufacturing and scientific laboratories largely stems from the prevalent use of organic solvents. Consequently, concerns regarding green chemistry and sustainability have prompted the rapid development of mechanochemical synthetic techniques that either minimize or entirely eliminate the need for organic solvents.

Drawing inspiration from mechanocatalysis techniques, we propose a novel approach for generating acyl radicals from aldehydes using the stainless-steel milling equipment as a replacement for the typical Fe catalyst used in homogeneous solutions. One of the key advantages of this strategy is that the stainless-steel ball employed in the ball milling process remains in the zero oxidation state, making it highly resistant to the influence of ambient atmosphere and water. In this study, we present the findings of a stainless-steel-initiated acylation reaction between quinoxalin-2(1H)-ones and aryl- and alkylaldehydes under ball milling conditions (Scheme 1c). This mechanocatalysis strategy demonstrated remarkable efficiency, providing a wide range of C3-acylated quinoxalin-2(1H)-ones in excellent yields within a short reaction time of 30 minutes. These results underscore the capability of stainless steel under ball milling conditions as a highly effective catalyst for Fe(0)-catalyzed reactions of this nature.

In the initial trials, 1-methylquinoxalin-2(1H)-one **1a** (0.2 mmol) and benzaldehyde **2a** (0.4 mmol) were used as model substrates to optimize the reaction conditions. The model

reaction was carried out in a 2 mL PE milling jar containing ten 3.5 mm stainless-steel balls as milling balls (MSK-SFM-12M mixer mill). To our delight, the desired product **3a** was obtained in 60% yield when using 30 mol% methanesulfonic acid (MSA), 10.0 equiv. of Celite as a solid grinding auxiliary, and 3.0 equiv. of TBHP as an oxidant (Table 1, entry 1). To be noticed, the commercially available TBHP as a 70% solution in water was used without further treatment. Other organic acids, including CH<sub>3</sub>COOH and trifluoroacetic acid (TFA), and inorganic acids, such as HCl and H<sub>2</sub>SO<sub>4</sub>, were screened (entries 2–5). The results showed that TFA was the optimal acid, providing the target product **3a** in excellent yield (93%). Reducing the amount of TFA or omitting the use of any acid resulted in a significant decrease in the product yield (entries 6 and 7), highlighting the essential role of acid in the successful transformation. Buoyed by these results, we further investigated the influence of other reaction reagents and parameters. Various oxidants, such as 3-chloroperbenzoic acid (*m*CPBA), *di-tert*-butyl peroxide (DTBP), *tert*-butyl peroxybenzoate (TBPB), MnO<sub>2</sub>, Na<sub>2</sub>S<sub>2</sub>O<sub>8</sub>, and K<sub>2</sub>S<sub>2</sub>O<sub>8</sub>, were compared with TBHP (entries 8–13). Organic peroxides, including *m*CPBA, DTBP, and TBPB, did not improve the yield of

Table 1 Optimization of the reaction conditions<sup>a</sup>

Entry	Acid (mol%)	Grinding reagent (equiv.)	Oxidant (equiv.)	Yield <sup>b</sup> (%)
1	MSA	Celite	TBHP	60
2	CH <sub>3</sub> COOH	Celite	TBHP	78
3	TFA	Celite	TBHP	93
4	HCl	Celite	TBHP	70
5	H <sub>2</sub> SO <sub>4</sub>	Celite	TBHP	75
6	TFA (10)	Celite	TBHP	60
7	—	Celite	TBHP	50
8	TFA	Celite	<i>m</i> CPBA	30
9	TFA	Celite	DTBP	15
10	TFA	Celite	TBPB	60
11	TFA	Celite	MnO <sub>2</sub>	Trace
12	TFA	Celite	Na <sub>2</sub> S <sub>2</sub> O <sub>8</sub>	15
13	TFA	Celite	K <sub>2</sub> S <sub>2</sub> O <sub>8</sub>	15
14	TFA	Celite	Oxone	17
15	TFA	Celite	—	Trace
16	TFA	Celite	TBHP (1.4)	94
17	TFA	Celite	TBHP (1.05)	50
18	TFA	Celite (1)	TBHP	94
19	TFA	Celite (0.5)	TBHP	94
20	TFA	Celite (0.2)	TBHP	90
21	TFA	Quartz sand	TBHP	90
22	TFA	Silica gel	TBHP	20
23	TFA	—	TBHP	Trace

<sup>a</sup> Reaction conditions: **1a** (0.2 mmol), **2a** (0.4 mmol), oxidant (2.1 equiv.), acid (30 mol%), grinding reagent (10 equiv.), 3800 rpm, twelve 3.5 mm 304 stainless-steel milling balls, air, 30 min. <sup>b</sup> Isolated yields.

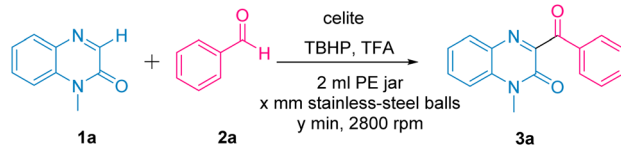


**3a** (entries 8–10). Similarly, inorganic oxidants such as  $\text{MnO}_2$ ,  $\text{Na}_2\text{S}_2\text{O}_8$ ,  $\text{K}_2\text{S}_2\text{O}_8$ , and oxone showed no efficacy in promoting the desired reaction (entries 11–14). A control experiment without any oxidant only resulted in a trace amount of the desired C3-acylation of quinoxalin-2(1*H*)-one, confirming the indispensable role of the oxidant in the oxidative coupling process (entry 15). Reducing the amount of TBHP from 2.1 equiv. to 1.4 equiv. had no significant impact on the product yield (entry 16). However, a further reduction in the amount of TBHP led to a decrease in the yield of **3a** (entry 17).

The addition of inert milling auxiliaries (*e.g.* Celite, silica gel, quartz sand, NaCl,  $\text{NaSO}_4$ , and basic or neutral  $\text{Al}_2\text{O}_3$ ) in stoichiometric amounts (1–5 equivalents) has been widely employed to enhance the reaction rate and performance of mechanochemical processes.<sup>18</sup> Although the precise mechanism behind this enhancement remains elusive, there are plausible explanations suggesting that these milling auxiliaries may act to ‘dilute’ the mechanochemical action, thereby influencing reaction kinetics. In light of this, we systematically investigated the quantity and type of the solid grinding assistant used in this oxidative coupling reaction. Notably, reducing the equivalent of Celite showed only a minor effect on the reactivity, and it was discovered that as little as 10 wt%. Celite was sufficient to promote the oxidative coupling reaction effectively under mechanochemical conditions (entries 18–20). Conversely, when Celite was replaced with sand or silica gel, a noticeable decrease in the yield of **3a** was observed (entries 21 and 22). Additionally, the complete removal of the milling auxiliary from the reaction system resulted in the absence of any product formation (entry 23). Based on these findings, we propose the hypothesis that the addition of Celite could create a more ‘powder-like’ milling environment, leading to enhanced mixing and homogeneity of the reaction mixture, consequently improving the reaction performance.

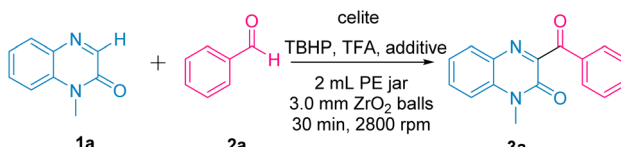
Subsequently, we conducted an evaluation of milling media, oscillating frequency, and ball-to-reagent mass ratio, as these crucial milling parameters can significantly impact the reaction kinetics and need to be optimized to achieve the most efficient mechanochemical reaction conditions. Lowering the oscillating speed from 3800 rpm to 2800 rpm (the lowest oscillating speed our ball mill could provide) showed no negative impact, yielding the product **3a** in 94% yield (Table 2, entry 1). Reducing the number of stainless-steel balls had a minimal effect on the yield (entries 2–5), while using fewer and heavier grinding balls still resulted in a favorable 90% yield (entry 6). Reaction time monitoring revealed that the reaction could achieve a remarkable 60% yield within just 6 minutes (entry 7). This result illustrates the impressive acceleration of the reaction and the reduction of the reaction period to merely minutes compared to the traditional solvent-based method.

It is prudent to consider the potential chemical leaching of metal ions from the stainless-steel milling balls, which could potentially influence the reaction outcome. To investigate this, we conducted experiments replacing the stainless-steel balls with  $\text{ZrO}_2$  balls, resulting in only a small amount of product generation (Table 3, entry 1). However, upon the addition of 10 mol% Fe powder to the  $\text{ZrO}_2$  milling ball system, the yield of the target

Table 2 Screening of mechanical parameters<sup>a</sup>


Entry	Ball size/mm (amount)	Time/min	Yield <sup>b</sup> /%
1	3.5 (12)	30	94
2	3.5 (10)	30	93
3	3.5 (8)	30	91
4	3.5 (6)	30	90
5	3.5 (4)	30	80
6	5.0 (6)	30	90
7	3.5 (12)	6	60
8	3.5 (12)	12	70
9	3.5 (12)	18	80
10	3.5 (12)	24	85
11	3.5 (12)	45	94

<sup>a</sup> Reaction conditions: **1a** (0.2 mmol), **2a** (0.4 mmol), TBHP (1.4 equiv.), TFA (30 mol%), Celite (10 wt%), 2800 rpm, x mm 304 stainless-steel milling balls, air, y min. <sup>b</sup> Isolated yields.

Table 3 Control experiments<sup>a</sup>


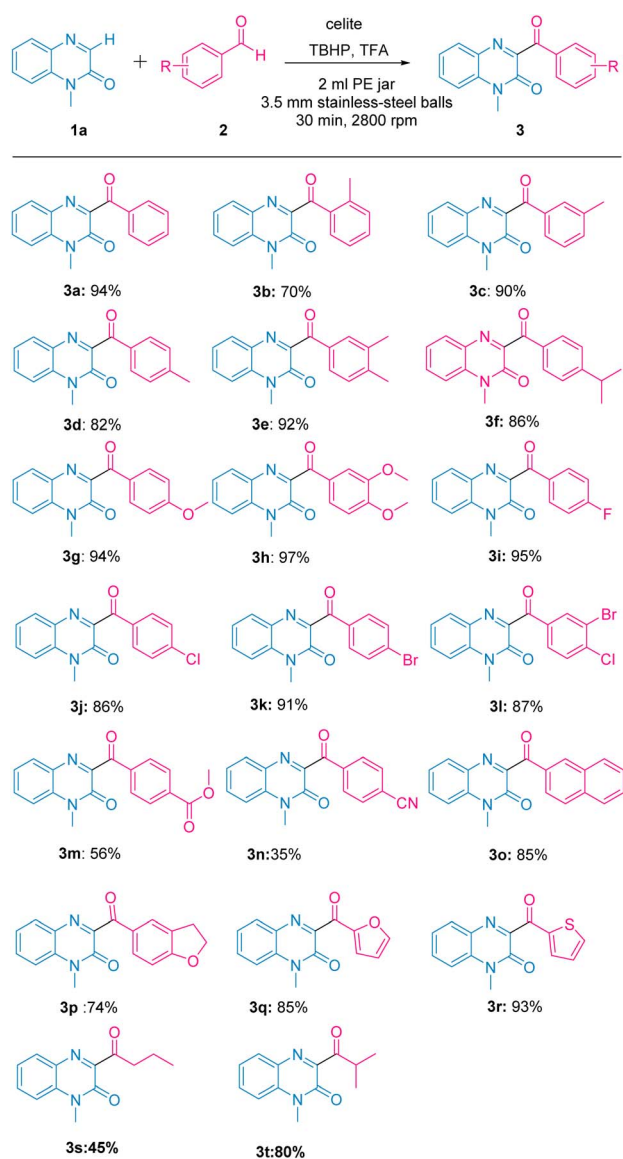
Entry	Additive (mol%)	Yield <sup>b</sup> (%)
1	—	Trace
2	Fe powder	60
3	Ni powder	8
4	Cr powder	Trace

<sup>a</sup> Reaction conditions: **1a** (0.2 mmol), **2a** (0.4 mmol), TBHP (1.4 equiv.), TFA (30 mol%), Celite (10 wt%), additive (10 mol%), 2800 rpm, twelve 3.0 mm  $\text{ZrO}_2$  milling balls, air, 2 mL PE jar, 30 min. <sup>b</sup> Isolated yields.

product significantly improved, reaching 60% (entry 2). Conversely, the addition of Ni powder or Cr powder separately in the  $\text{ZrO}_2$  milling ball system did not lead to any improvement in the target product yield (entries 3 and 4). These results suggest that the presence of Fe powder could play a beneficial role in enhancing the reaction efficiency under these conditions.

After optimizing the reaction conditions, we explored the substrate scope of various aryl aldehydes (Table 4). A wide range of aromatic aldehydes bearing both electron-donating and electron-withdrawing groups were examined. Aldehydes with single or multiple electron-donating groups, including methyl (**3b–e**), isopropyl (**3f**), and methoxy (**3g**, **3h**) groups, and electron-withdrawing groups, such as halogen (**3i–l**) and ester (**3m**) groups, provided the corresponding products in modest to



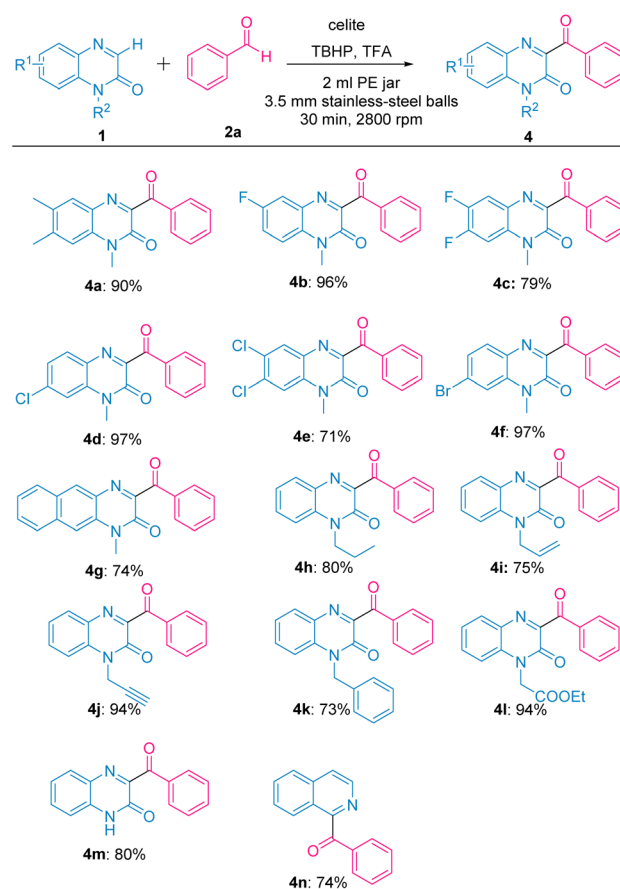
Table 4 The substrate scope of aldehyde<sup>a,b</sup>

<sup>a</sup> Reaction conditions: 1a (0.2 mmol), 2 (0.4 mmol), TBHP (1.4 equiv.), TFA (30 mol%), Celite (0.5 equiv.), 2800 rpm, twelve 3.5 mm 304 stainless-steel balls, air, 30 min. <sup>b</sup> Isolated yields.

excellent yields. The steric hindrance effect of substitution on the phenyl ring of aromatic aldehydes played a role in the oxidative coupling reaction; for example, *ortho*-methyl substitution resulted in a relatively lower product yield compared to *meta*- or *para*-substituted substrates (3b–d). In the presence of strong electron-withdrawing groups like cyano, the corresponding product 3n was obtained in a lower yield of 35%. 2-Naphthaldehyde, 2,3-dihydrobenzofuran-5-carbaldehyde, and heterocyclic aromatic aldehydes, including 2-furfural and 2-thiophenealdehyde, were well tolerated, yielding the desired products 3o–r in good yields. Furthermore, the reaction between 1a and aliphatic aldehyde proceeded smoothly using the current protocol, providing the desired products 3s and 3t in moderate to good yields.

To further explore the substrate scope and limitations of this protocol, a broad range of quinoxalin-2(1H)-ones containing various electron-donating and electron-withdrawing groups were investigated (Table 5). Quinoxalin-2(1H)-ones with methyl, fluoro, chloro, and bromo substituents provided the desired C3-acylated products in good to excellent yields (4a–f). Additionally, we screened *N*-substituted functional groups on quinoxalin-2(1H)-one. The presence of propyl, allyl, benzyl, propynyl, and ester groups proved to be compatible, delivering products (4h–l) in excellent yields. The *N*-unsubstituted quinoxalin-2(1H)-one showed good compatibility with these reaction conditions as well, giving product 4m in 80% yield. Moreover, we extended our investigation to other *N*-heterocyclic aromatic compounds, such as isoquinoline, which could be efficiently converted into the desired acylated isoquinoline (4n) in excellent yield under these conditions.

To further demonstrate the practicability of this acylation reaction, we explored the modification of pharmaceutical-related compounds (Fig. 1a). The quinoxalin-2(1H)-one derivative 5, incorporating an ibuprofen motif, efficiently yielded the corresponding product 5a under the given reaction conditions. Additionally, we calculated the *E*-factor to assess the

Table 5 The substrate scope of quinoxalin-2(1H)-ones<sup>a,b</sup>

<sup>a</sup> Reaction conditions: 1 (0.2 mmol), 2a (0.4 mmol), TBHP (1.4 equiv.), TFA (30 mol%), Celite (10 wt%), 2800 rpm, twelve 3.5 mm 304 stainless-steel balls, air, 30 min. <sup>b</sup> Isolated yields.



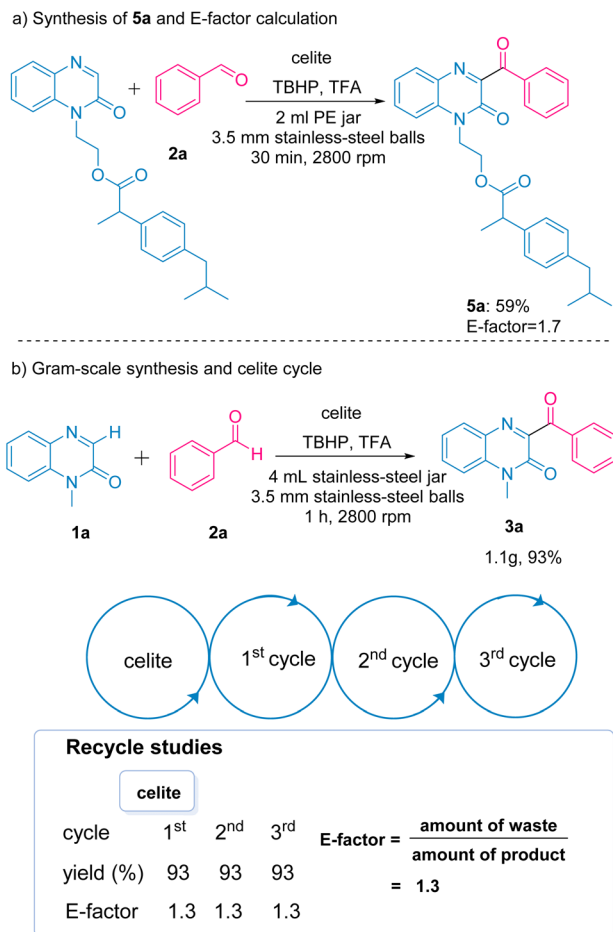


Fig. 1 (a) *E*-factor calculation for **5a**. (b) Gram scale synthesis of **3a** and recycle study.

sustainability and high atom economy of this reaction, yielding an *E*-factor of 1.7, which compares favorably with other solution methods (see the ESI† for more details).

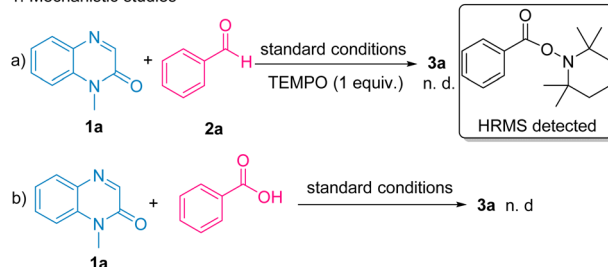
Moreover, we conducted a study on the gram-scale synthesis of compound **3a** in an ST-M200 mill (a 4 mL stainless-steel grinding tank with twenty 3.5 mm stainless-steel grinding balls at 2200 rpm). To our delight, the gram-scale C3 acylation of 1-methylquinoxalin-2(1*H*)-one **1a** with benzaldehyde **2a** successfully provided the target product **3a** in 93% yield (Fig. 1). Notably, we also adopted a recycling approach for the grinding reagent in gram-scale reactions. The Celite from the crude reaction mixture was separated, washed, and dried. It was used for the next run of the mechanochemical acylation by adding a fresh batch of reactants and acid for each cycle. To our satisfaction, the Celite could be reused three times without reducing the product yield (Fig. 1), and the *E*-factor is as low as 1.3 (see the ESI† for more details), further corroborating the eco-friendly nature of our approach. The recyclable Celite can undoubtedly be reused more times, but researchers need to consider the recovery loss during the work-up procedure, which may limit its reusable times.

We hypothesized that the benzaldehyde acylation reactions involved radical species, and to investigate the reaction

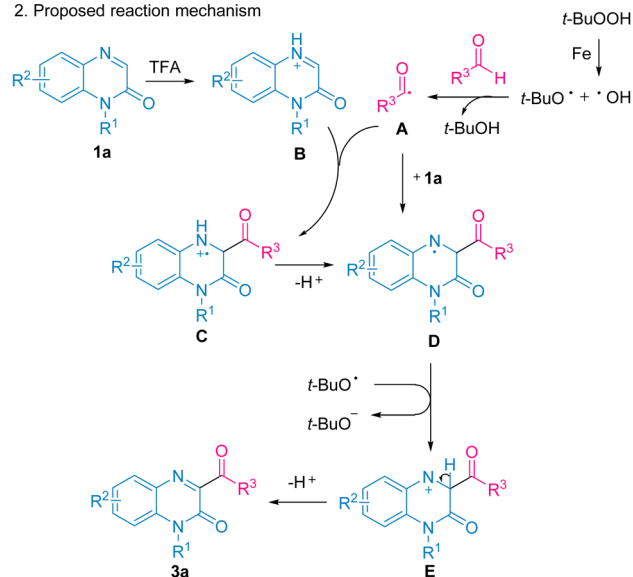
mechanism, we conducted control experiments. When 1 equivalent of TEMPO (2,2,6,6-tetramethyl-1-piperidinyloxy) was used as a radical inhibitor, the reaction was sufficiently suppressed (Scheme 2, reaction 1a). HRMS analysis of the reaction mixture confirmed the presence of the radical trapped adduct of benzoyl radical, providing evidence for the involvement of free radical intermediates. On the other hand, when benzoic acid was used as the substrate under standard conditions, no conversion of **3a** was observed (Scheme 2, reaction 1b), ruling out the involvement of the benzoic acid intermediate.

It is well established that Fe salts promote the homolytic cleavage of TBHP, generating a *tert*-butoxy radical and a hydroxyl radical under heating. In our reaction, Fe, present in the stainless-steel milling equipment, acts as a catalyst to accelerate the homolytic cleavage of TBHP. The *tert*-butoxyl radical then abstracts a hydrogen atom from the aldehyde, leading to an acyl radical **A**. Acyl radical **A** and protonated quinoxalin-2(1*H*)-one **B** undergo a radical addition reaction to form a radical cation intermediate **C**, which subsequently loses a proton to generate a free radical intermediate **D**. Alternatively, acyl radical **A** can directly attack the C3 position of quinoxalin-2(1*H*)-one **1a** to form free radical intermediate **D**. Next, intermediate **D** reacts with the *tert*-butoxyl radical, resulting in the formation of nitrogen cation intermediate **E**. Finally, intermediate **E** deprotonates to yield the target product **3a**.

#### 1. Mechanistic studies



#### 2. Proposed reaction mechanism



Scheme 2 Mechanistic studies and proposed reaction mechanism.



## Conclusions

In conclusion, we developed a mechanochemical acylation reaction of quinoline-2(1*H*)-one with aldehydes initiated by stainless-steel balls. This mechanochemical protocol could avoid using potentially harmful organic solvents, shortens reaction periods into minutes, and simplifies operational handling (reaction carried out under an ambient atmosphere). Fe present in the stainless-steel milling equipment acts as a catalyst to promote the homolytic cleavage of TBHP. The generated radicals facilitate the formation of acyl radicals and subsequently lead to the desired product formation in a short reaction period. This mechanistic understanding of the reaction provides valuable insights into the role of Fe(0) in the catalytic process and contributes to the development of effective and sustainable acylation protocols using mechanochemical techniques. The practicality of this protocol has been demonstrated through gram-scale synthesis and Celite cycling experiments, making it applicable for larger-scale production. The combination of high yields, scalability, and recyclability of the milling auxiliary strengthens the viability of this approach as a valuable tool in green and efficient organic synthesis.

## Data availability

The data supporting this article have been included as part of the ESI.†

## Conflicts of interest

The authors declare no conflicts of interest.

## Acknowledgements

This work was financially supported by the National Natural Science Foundation of China (No. 21801229), Key-Area Research and Development Program of Guangdong Province (No. 2020B010188003), and Natural Science Foundation of Henan Province (No. 222300420528).

## References

- (a) R. R. A. Bolt, J. A. Leitch, A. C. Jones, W. I. Nicholson and D. L. Browne, *Chem. Soc. Rev.*, 2022, **51**, 4243–4260; (b) I. N. Egorov, S. Santra, D. S. Kopchuk, I. S. Kovalev, G. V. Zyryanov, A. Majee, B. C. Ranu, V. L. Rusinov and O. N. Chupakhin, *Green Chem.*, 2020, **22**, 302–315; (c) Q. Cao, D. E. Crawford, C. Shi and S. L. James, *Angew. Chem., Int. Ed.*, 2020, **59**, 4478–4483; *Angew. Chem.*, 2020, **132**, 4508–4513; (d) J. L. Howard, Q. Cao and D. L. Browne, *Chem. Sci.*, 2018, **9**, 3080–3094; (e) D. Tan and F. Garcia, *Chem. Soc. Rev.*, 2019, **48**, 2274–2292.
- (a) S. Ni, M. Hribersek, S. K. Baddigam, F. J. L. Ingner, A. Orthaber, P. J. Gates and L. T. Pilarski, *Angew. Chem. Int. Ed.*, 2021, **60**, 6660–6666; *Angew. Chem.*, 2021, **133**, 6734–6740; (b) F. Krauskopf, K. N. Truong, K. Rissanen and C. Bolm, *Org. Lett.*, 2021, **23**, 2699–2703; (c) A. Porcheddu, E. Colacino, L. De Luca and F. Delogu, *ACS Catal.*, 2020, **10**, 8344–8394; (d) M. Đud, A. Briš, I. Jušinski, D. Gracin and D. Margetić, *Beilstein J. Org. Chem.*, 2019, **15**, 1313–1320; (e) E. Troschke, S. Grätz, T. Lübken and L. Borchardt, *Angew. Chem., Int. Ed.*, 2017, **56**, 6859–6863; (f) A. Krusenbaum, S. Grätz, G. T. Tigineh, L. Borchardt and J. G. Kim, *Chem. Soc. Rev.*, 2022, **51**, 2873–2905.
- (a) M. Pérez-Venegas and E. Juaristi, *ACS Sustain. Chem. Eng.*, 2020, **8**, 8881–8893; (b) A. A. L. Michalchuk, E. V. Boldyreva, A. M. Belenguer, F. Emmerling and V. V. Boldyrev, *Front. Chem.*, 2021, **9**, 685789–685818; (c) F. Shen, X. Xiong, J. Fu, J. Yang, M. Qiu, X. Qi and D. C. W. Tsang, *Renewable Sustainable Energy Rev.*, 2020, **130**, 109944–109964; (d) S. L. James, C. J. Adams, C. Bolm, D. Braga, P. Collier, T. Frišić, F. Grepioni, K. D. M. Harris, G. Hyett, W. Jones, A. Krebs, J. Mack, L. Maini, A. G. Orpen, I. P. Parkin, W. C. Shearouse, J. W. Steed and D. C. Waddell, *Chem. Soc. Rev.*, 2012, **41**, 413–447; (e) A. L. Garay, A. Pichon and S. L. James, *Chem. Soc. Rev.*, 2007, **36**, 846–855.
- D. A. Fulmer, W. C. Shearouse, S. T. Medonza and J. Mack, *Green Chem.*, 2009, **11**, 1821–1825.
- C. G. Vogt, S. Gratz, S. Lukin, I. Halasz, M. Etter, J. D. Evans and L. Borchardt, *Angew. Chem., Int. Ed.*, 2019, **58**, 18942–18947; *Angew. Chem.*, 2019, **131**, 19118–19123.
- R. A. Haley, A. R. Zellner, J. A. Krause, H. Guan and J. Mack, *ACS Sustain. Chem. Eng.*, 2016, **4**, 2464–2469.
- W. Su, J. Yu, Z. Li and Z. Jiang, *J. Org. Chem.*, 2011, **76**, 9144–9150.
- (a) D. Kong and C. Bolm, *Green Chem.*, 2022, **24**, 6476–6480; (b) J. Gómez-Carpintero, C. Cabrero, J. D. Sánchez, J. F. González and J. C. Menéndez, *Green Chem. Lett. Rev.*, 2022, **15**, 639–645.
- (a) Y. Sawama, M. Niikawa, Y. Yabe, R. Goto, T. Kawajiri, T. Marumoto, T. Takahashi, M. Itoh, Y. Kimura, Y. Sasai, Y. Yamauchi, S.-i. Kondo, M. Kuzuya, Y. Monguchi and H. Sajiki, *ACS Sustain. Chem. Eng.*, 2015, **3**, 683–689; (b) Y. Sawama, N. Yasukawa, K. Ban, R. Goto, M. Niikawa, Y. Monguchi, M. Itoh and H. Sajiki, *Org. Lett.*, 2018, **20**, 2892–2896.
- K. Martina, F. Baricco, S. Tagliapietra, M. J. Moran, G. Cravotto and P. Cintas, *New J. Chem.*, 2018, **42**, 18881–18888.
- D. Kong, M. M. Amer and C. Bolm, *Green Chem.*, 2022, **24**, 3125–3129.
- (a) L. Biesen and T. J. J. Müller, *Adv. Synth. Catal.*, 2021, **363**, 980–1006; (b) G. Yashwantrao and S. Saha, *Org. Chem. Front.*, 2021, **8**, 2820–2862; (c) L.-Y. Xie, Y.-S. Bai, X.-Q. Xu, X. Peng, H.-S. Tang, Y. Huang, Y.-W. Lin, Z. Cao and W.-M. He, *Green Chem.*, 2020, **22**, 1720–1725; (d) X. Qin, X. Hao, H. Han, S. Zhu, Y. Yang, B. Wu, S. Hussain, S. Parveen, C. Jing, B. Ma and C. Zhu, *J. Med. Chem.*, 2015, **58**, 1254–1267; (e) S. A. Galal, S. H. Khairat, F. A. Ragab, A. S. Abdelsamie, M. M. Ali, S. M. Soliman, J. Mortier, G. Wolber and H. I. El Diwani, *Eur. J. Med. Chem.*, 2014, **86**, 122–132; (f) V. A. Mamedov, A. A. Kalinin, A. T. Gubaidullin, I. A. Litvinov and Ya. A. Levin, *Russ. J. Org. Chem.*, 2006, **42**, 1532–1543; (g) V. A. Mamedov, A. A. Kalinin,



- A. T. Gubaidullin, I. A. Litvinov and Ya. A. Levin, *Chem. Heterocycl. Compd.*, 2022, **38**, 1504–1510; (h) V. A. Mamedov, A. A. Kalinin, A. T. Gubaidullin, O. G. Isaikina and I. A. Litvinov, *Russ. J. Org. Chem.*, 2005, **41**, 599–606.
- 13 (a) K. C. C. Aganda, B. Hong and A. Lee, *Adv. Synth. Catal.*, 2021, **363**, 1443–1448; (b) M. Weiwer, J. Spoonamore, J. Wei, B. Guichard, N. T. Ross, K. Masson, W. Silkworth, S. Dandapani, M. Palmer, C. A. Scherer, A. M. Stern, S. L. Schreiber and B. Munoz, *ACS Med. Chem. Lett.*, 2012, **3**, 1034–1038; (c) J. Lu, X. K. He, X. Cheng, A. J. Zhang, G. Y. Xu and J. Xuan, *Adv. Synth. Catal.*, 2020, **362**, 2178–2182.
- 14 (a) W. C. Yang, J. G. Feng, L. Wu and Y. Q. Zhang, *Adv. Synth. Catal.*, 2019, **361**, 1700–1709; (b) Y. Zhang, P. Ji, Y. Dong, Y. Wei and W. Wang, *ACS Catal.*, 2020, **10**, 2226–2230; (c) M.-S. Liu, L. Min, B.-H. Chen and W. Shu, *ACS Catal.*, 2021, **11**, 9715–9721; (d) J. Yan, H. Tang, E. J. R. Kuek, X. Shi, C. Liu, M. Zhang, J. L. Piper, S. Duan and J. Wu, *Nat. Commun.*, 2021, **12**, 7214–7224; (e) Y. L. Liu, Y. J. Ouyang, H. Zheng, H. Liu and W. T. Wei, *Chem. Commun.*, 2021, **57**, 6111–6120.
- 15 L. Ge, Y. Li and H. Bao, *Org. Lett.*, 2019, **21**, 256–260.
- 16 C. S. Wu, R. X. Liu, D. Y. Ma, C. P. Luo and L. Yang, *Org. Lett.*, 2019, **21**, 6117–6121.
- 17 J. Yuan, J. Fu, S. Liu, Y. Xiao, P. Mao and L. Qu, *Org. Biomol. Chem.*, 2018, **16**, 3203–3212.
- 18 P. Ying, J. Yu and W. Su, *Adv. Synth. Catal.*, 2021, **363**, 1246–1271.

